Two-Dimensional Simulation of Ferroelectric Memory Cells

Klaus Dragosits and Siegfried Selberherr, *Fellow, IEEE*

***Abstract*—An approach to increase the capabilities of integrated circuit nonvolatile memory is to take advantage of the hysteresis in the polarization of ferroelectric materials. For a rigorous analysis of the resulting devices, a suitable model for the ferroelectric effects has been developed. We present this model and show the results of its implementation into a device simulator. Although this model was designed especially for analysis of ferroelectric materials, it is also applicable to magnetic hysteresis phenomena.**

***Index Terms*—Ferroelectric materials, hysteresis, nonvolatile memory.**

I. Introduction

THE development of nonvolatile memory cells using ferroelectric materials leads to designs with two-dimensional (2-D) geometries like the finger structure outlined in Fig. 1.

The generic approach of MINIMOS-NT [1] makes it possible to simulate structures with an arbitrary number of contacts on an almost arbitrary configuration of different materials. To account for the simulation of ferroelectric materials, a useful algorithm has to consider not only the 2-D field distribution but also the occurrence of field rotation.

Considering the fact that hysteresis depends on the previous operating points, field rotation is a nontrivial problem, e.g., as described by [2] and [3] in the context of magnetism, a constant rotation of the electric field leads to a lag angle of the induction.

Aside from calculating the exact field distribution a simulator for ferroelectric devices has to fulfill further requirements: To allow the calculation of transfer characteristics it has to be insensitive to the magnitude of the applied voltage steps. And, to keep pace with future developments of ferroelectric devices, the extension of the algorithm to three dimensions should be possible.

II. The Simulation Model

Ferroelectric hysteresis influences the electric displacement $\vec{D}$. We separate it into a linear and a nonlinear part:

$$\vec{D} = \epsilon \cdot \vec{E} + \vec{P}. \tag{1}$$

The nonlinear part $\vec{P}$ holds the hysteresis and is modeled by

$$P = k \cdot f(E \pm E_c, k) + P_{off}. \tag{2}$$

Manuscript received July 14, 1999; revised September 1, 2000. This work is supported by Siemens/Infineon EZM, Villach, Austria and Siemens AG/Infineon Munich, Germany. The review of this paper was arranged by Editor A. H. Marshak.

The authors are with the Institute for Microelectronics, Technische Universität Wien, A-1040, Vienna, Austria (e-mail: dragosits@iue.tuwein.ac.at).

Publisher Item Identifier S 0018-9383(01)00774-2.

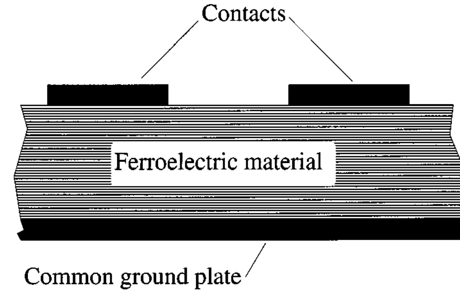

Fig. 1. Cross section of a finger structure.

The parameters k and P_{off} are necessary for the simulation of the locus curves of the hysteresis, the function f is the shape function for these locus curves, E_c is the coercive field of the material. We assume that on each grid point the hysteresis properties can be modeled with this macroscopic approach. This might seem a big simplification because it does not consider the well known domain structure of ferroelectric materials. However, a simulation including this effect would need a very accurate description of the device, including parameters like the exact contribution of the defects in the crystal lattice, which are usually not available, or the grain distribution. Furthermore it will only deliver the results for this special device. So the basic aim of our approach is not the simulation of a singular device but to approximate the average behavior of devices with the specified geometry.

Starting from (2) a 2-D algorithm had to be developed to calculate the polarization vector $\vec{P}$ and the resulting electric displacement $\vec{D}$.

A. Polarization in an Orthogonal Direction

The basic key to develop a rigorous approach to 2-D hysteresis is to find a useful formulation for the following problem: We assume a piece of ferroelectric material with a remanent polarization $\vec{P}_{rem}$. Now an electric field is applied in the perpendicular direction.

The newly applied electric field raises a polarization component $P_{||}$ in the same direction, plotted in Fig. 2. Regarding the fact that there was no polarization in this direction, an initial polarization curve (dashed line) is used. The limited number of dipoles introduces the saturation polarization as a hard limit. This means that it is not possible to achieve saturation in the direction of the applied field without any consequence for the initial component $\vec{P}_{rem}$. So we can formulate

$$||\vec{P}_{rem} + \vec{P}_{||}|| \leq P_{Sat} \tag{3}$$

0018–9383/01$10.00 © 2001 IEEE

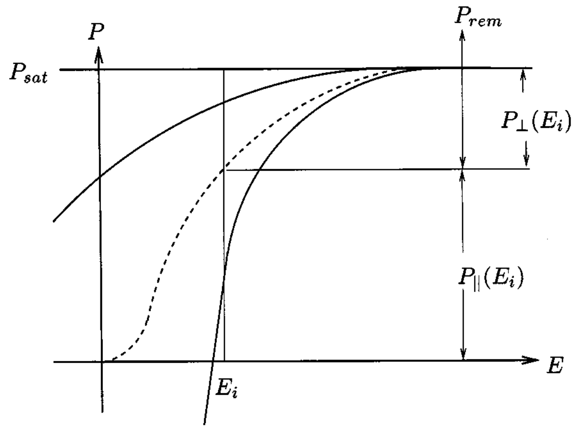

Fig. 2. Construction of the polarization components.

as hard limit to the resulting polarization.

Regarding the domain structure of the material and assuming the rotation of dipoles to be impossible, the sum of magnitudes of the newly raised and the remanent component will not exceed the saturation:

$$||\vec{P}_{rem}|| + ||\vec{P}_{||}|| \leq P_{Sat}. \quad (4)$$

Note that even in the case that (4) does not fulfill the exact physical properties, a similar more general constraint of the form

$$||\vec{P}_{rem}|| + ||\vec{P}_{||}|| \leq f(||\vec{E}||) \quad (5)$$

must be satisfied.

For our model we assume, that, if the chosen constraint is not fulfilled, the component $||\vec{P}_{rem}||$ will be reduced, due to the fact that there is no field component in this direction. The resulting polarization is plotted in Fig. 3.

B. General 2-D Algorithm

The basic principle of our model is to split the polarization $\vec{P}_{old}$ and the electric field $\vec{E}_{old}$ of the previous operating point into the components in the direction of the next applied electric field $\vec{E}_1$, leading to $\vec{P}_{old,||}$ and $\vec{E}_{old,||}$ as well as orthogonal $\vec{P}_{old,\perp}$ and $\vec{E}_{old,\perp}$ (Fig. 4).

Making use of this projections, we separate the 2-D problem into two one-dimensional (1-D) problems. The equation

$$(P_{||,0}, E_{||,0}) \rightarrow (P_{||,1}, E_1) \quad (6)$$

denotes the problem in the direction of the electric field. The second problem in the orthogonal direction can be described as

$$(P_{\perp,0}, E_{\perp,0}) \rightarrow (P_{\perp,1}, 0). \quad (7)$$

For each of these components a locus curve is calculated. These are outlined in Fig. 5.

The component $\vec{P}_{||,1}$ in the direction of the electric field is calculated by entering the signed length of the electric field vector into the equation of the locus curve. The actual algorithm to achieve this quantity will be discussed in Section III-A. The argument for the locus curve in the orthogonal direction is, according to the geometrical properties, zero. Therefore we

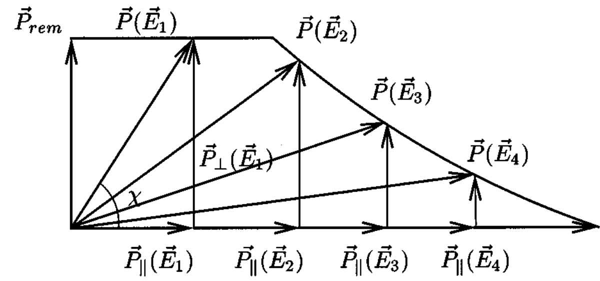

Fig. 3. Construction of the lag angle.

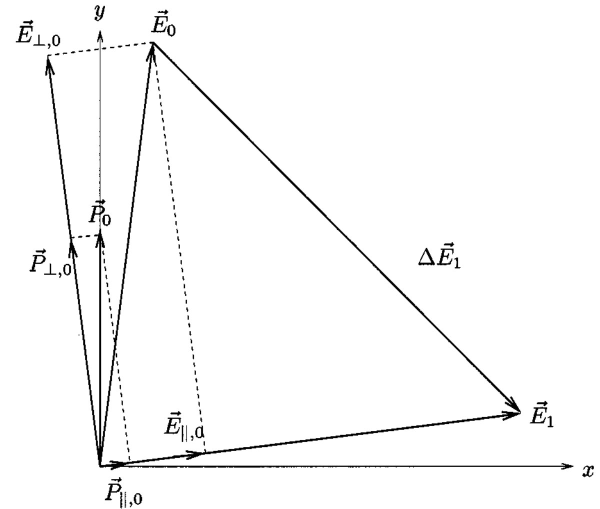

Fig. 4. Splitting of the field vectors.

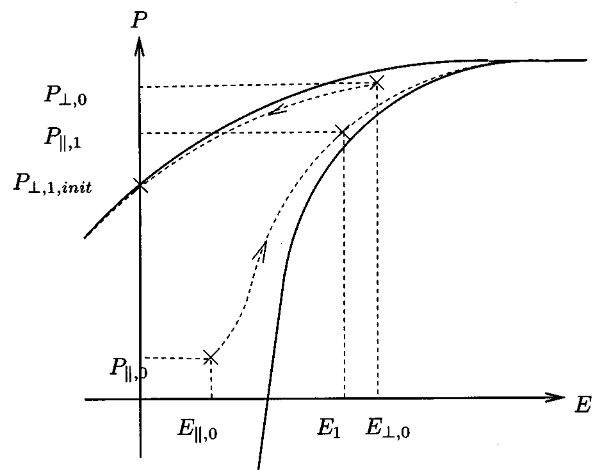

Fig. 5. Calculation of the initial guess.

achieve a remanent polarization for the component $\vec{P}_{\perp,1,init}$ into that direction. These two polarization components are forming a primary guess $\vec{P}_{init}$ for the next polarization, plotted in Fig. 6.

Due to the vanishing electric field in the normal direction we apply the criterion (4): Component $\vec{P}_{\perp}$ is reduced appropriately with respect to this limit. This is shown schematically in Figs. 7 and 6 and leads to the actual polarization vector $\vec{P}_1$ and the lag angle χ.

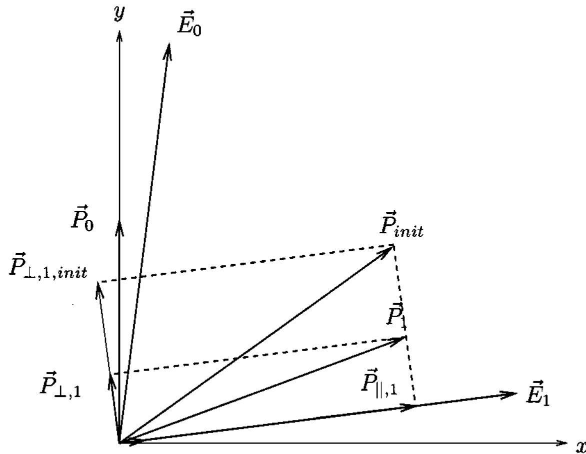

Fig. 6. Calculation of the polarization.

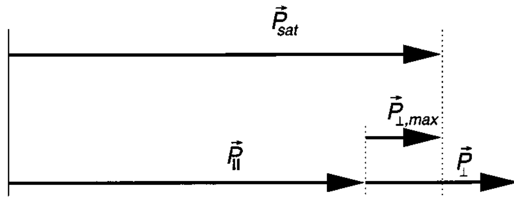

Fig. 7. Reduction of the orthogonal component.

As a first approach to the upper limit in the available number of switching dipoles the saturation polarization $\vec{P}_{sat}$ was considered, but the simulator is already prepared to use any function of the magnitude of the applied electric field $||\vec{E}||$. The algorithm to handle field rotation is also applicable for the nontrivial analysis of 3-D problems.

III. Numeric Implementation

Using the algorithm outlined above the box integration method is applied and Poisson's equation

$$div\vec{D} = \rho \tag{8}$$

is solved. As a consequence of the general approach, the following numerical aspects have to be considered in order to allow a 2-D simulation:

- nonsymmetry of the locus curves;
- influence of previous operating points;
- selection of the shape of the hysteresis curve;
- detection of the correct locus curve.

A. Nonsymmetry of the Locus Curves

In the last section we outlined a method to reduce the 2-D problem into two one-dimensional ones. But still the 1-D representations of the field quantities have to be found. This demands an extension to common discretizations, because in contrast to most of the functions used in device simulation, the locus curves of the hysteresis are nonsymmetric functions. The mere calculation of the vector length is not sufficient, also a criterion for the sign has to be established. Accordingly, the orientation of the field vector compared with the box boundary becomes decisive for the sign of the function argument. Furthermore, as a consequence of the hysteresis properties, it cannot be assumed that the sign of the resulting flux of the electric displacement is the same as for the applied electric field.

B. Influence of the Previous Operating Points

The calculation of the current locus curves uses the parallel and orthogonal component of the previously applied fields in respect to the current electric field. This is a major difference to 1-D simulation which only requires the storage of selected turning points [4]. In order to deal with this information in a suitable way, it is necessary to make adjustments to the field discretization. It is intuitive that the history information is required on the box boundary and that it cannot be derived from a representation in the grid points alone, as it is suitable for non hysteretic properties [5].

C. Selection of the Shape of the Hysteresis Curve and History Management

For a general approach to two-dimensional hysteretic effects an inhomogeneous field distribution has to be assumed. Therefore, a different locus curve has to be calculated on each box boundary. To keep the computational effort reasonable, it is necessary to chose analytic functions. By now two different types of shape functions have been investigated, the $\tanh$ and the $\arctan$ function. The first implementation is

$$P = k \cdot P_{sat} \cdot \tanh(w \cdot (E \pm E_c)) + P_{off}. \tag{9}$$

w is a shape parameter and the same for each locus curve. This function is a good approach for the simulation of PZT($Pb(Zr,Ti)O_3$). The second is the $\arctan$ shaped function

Again, w is the shape parameter. The $\arctan$ function covers the physical properties of SBT($SrBi_2Ta_2O_9$) in a very accurate way. It has to be noted that the locus parameters have to be calculated numerically, which leads to higher numerical effort.

Using these locus curves, the whole history of the ferroelectric material is simulated. The parameters of the locus curves are calculated according to Preisach hysteresis [6]. This includes the simulation of the following effects.

- *Locus curves hit last turning point*: This allows the simulation of closed subcycles.
- *Memory wipe out*: Turning point erases all information of previous smaller turning points.

A complete set of locus curves is plotted in the example Section IV-A, in Fig. 12, and the following. The figures show the simulation results for a planar capacitor.

D. Detection of the Locus Curve

A sophisticated task is to calculate the locus curves for a new operating point. As outlined in Fig. 8 one of two possible locus curves has to be chosen at each operating point, depending on the history of the electric field [4].

As a consequence of the 2-D algorithm the common starting point C of these two branches will move during the nonlinear

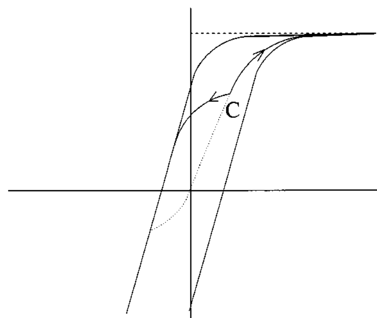

Fig. 8. Possible locus curves in an operating point.

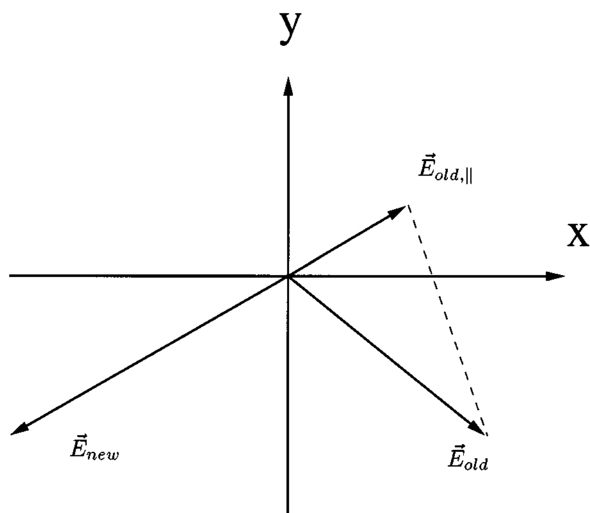

Fig. 9. Detection of the change of the electric field, electric field decreases.

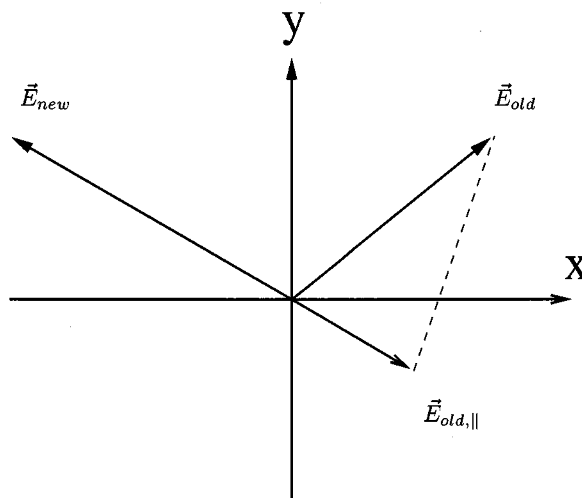

Fig. 10. Detection of the change of the electric field, electric field increases.

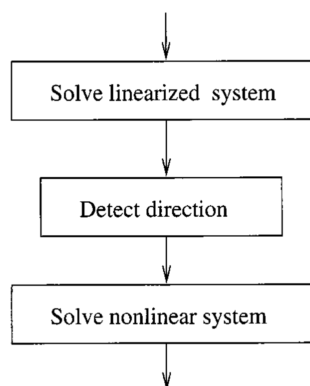

Fig. 11. Modified trivial iteration scheme.

iteration. In fact, it highly depends on the assumed electric field. Therefore, it cannot be guaranteed that the same branch is selected at each iteration step. Regarding the different derivatives of the two functions this will lead to poor convergence and in worst case to oscillations of the nonlinear iteration.

As practice shows a preselection of the correct branch is necessary to achieve good convergence, especially for the simulation of complex structures. A suitable approach to detect the direction of the change of the electric field is to solve a linearized equation system. In this system the nonlinear part of the displacement is kept constant and only the linear part is modified. Using this method an approximation to the electric field in the new operating point is derived.

Based on this information, it has to be decided whether the electric field was increased or not. The straightforward approach to compare the absolute values of the old and the new electric field will obviously fail, even if the two field vectors are parallel. For the applied algorithm the parallel component of the old field vector is calculated, and the result is interpreted in dependence of the orientation of the new field vector as outlined in Figs. 9 and 10. With this information it is now possible to select the correct branch of the hysteresis curve. The complete scheme is outlined in Fig. 11.

IV. Simulation Results

In order to check the abilities of our model, several devices have been simulated. The first two of the following examples were calculated with $\arctan$ shape functions. The ferroelectric memory field effect transistor (FEMFET) was analyzed with $\tanh$ functions.

A. Simulation of a Simple Capacitor

To allow the comparison with existing simulators, which use a compact model, a 1-D example has been calculated. The 1-D behavior of the device is a consequence of its planar structure and the applied boundary condition, which does not allow any field components outside of the device.

The resulting Q–V characteristics are plotted above in Fig. 12. Figs. 13 and 14 show the current response of the device and the actually applied input voltage. As expected, the 2-D algorithm of MINIMOS-NT is able to reproduce the one-dimensional properties correctly.

B. Simulation of a Finger Structure

C. Simulation of a FEMFET

The finger structure, outlined in Fig. 1 shows properties and effects that exceed the one-dimensional case. As a result of the

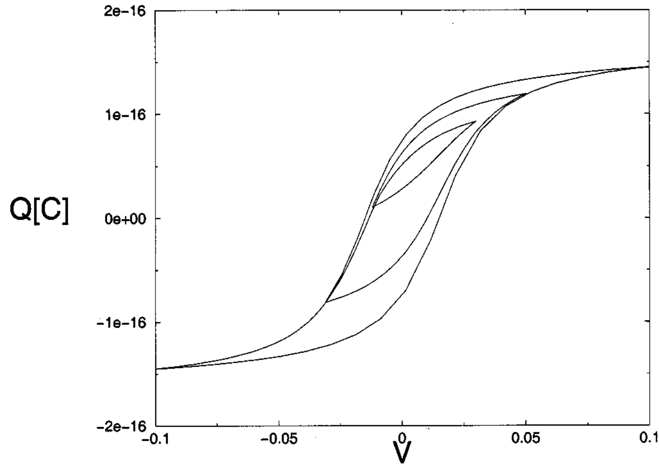

Fig. 12. *Q–V* Characteristics of a planar "1-D" capacitor.

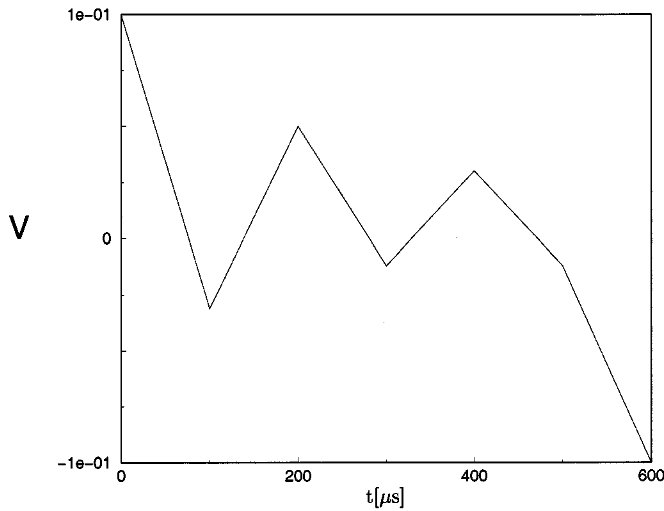

Fig. 13. Applied voltage to the "1-D" capacitor.

well known edge effect of the electric field, the polarization will be near saturation in these areas, even if small voltages are applied. For our first simulation we reduced the scope to the area marked in Fig. 15. Fig. 16 shows the simulated *Q–V* characteristic of this 2-D device and compares it to the result of the simple 1-D structure. With these simulation results it is possible to extract new hysteresis parameters for a compact model which allow the appropriate simulation of this 2-D structure. The resulting *Q–V* characteristics of this calibration are outlined in Fig. 17.The FEMFET is a device based on the hysteretic properties of the polarization and the displacement of a ferroelectric material. The FEMFET was constructed by inserting a ferroelectric segment in the subgate area of an NMOS, as outlined in Fig. 18. The threshold voltage of the NMOS was 0.7 V, its gate length was 0.18 μm. In consequence to the higher polarization, the threshold voltage of the FEMFET was reduced to 0.6 V. According to Poisson's equation the displacement influences the charge at the surface of the substrate. The ferroelectric polarization increases the displacement and leads to a significantly higher space charge density in the channel area. The different contributions of the space charge density of the NMOS transistor and the FEMFET were calculated and are plotted in Figs. 19 and 20, respectively. This causes a higher drain current of the FEMFET for the same gate voltage. As a result of the the hysteretic behavior of the polarization the drain current of the

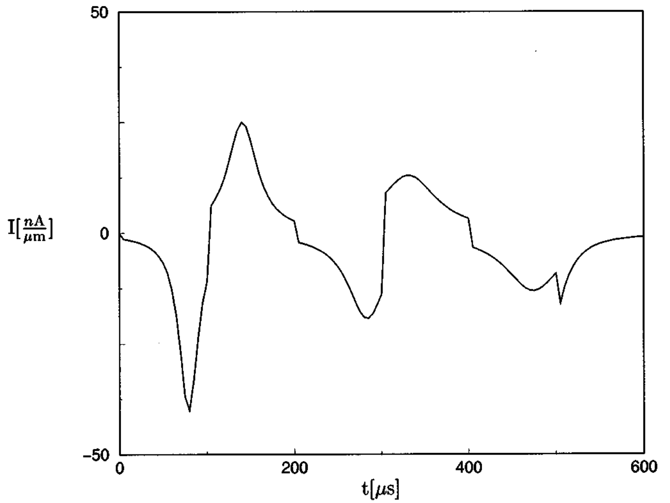

Fig. 14. Current response of the "1-D" capacitor.

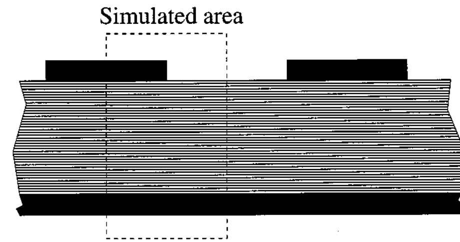

Fig. 15. Cross section of a finger structure and simulated area.

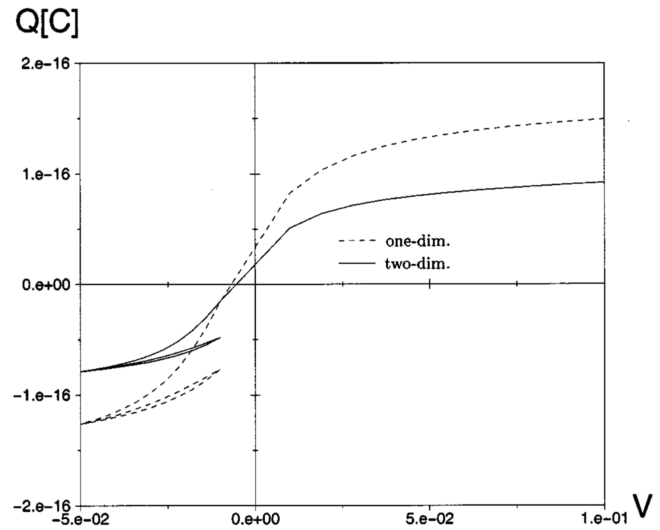

Fig. 16. "One-dimensional" capacitor versus finger structure.

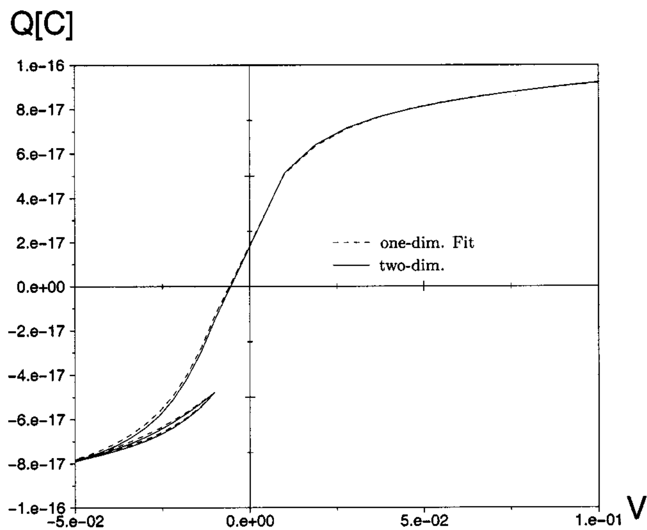

Fig. 17. Comparison of the transfer characteristics of a finger structure and the "1-D" capacitor with fitted hysteresis parameters.

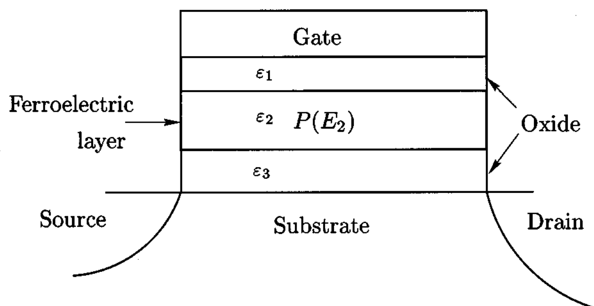

Fig. 18. Ferroelectric nonvolatile memory field effect transistor.

device does not only depend on the gate voltage but also on the history of the gate voltage. So the current–voltage (*I–V*) characteristics of the transistor show also a hysteresis which allows the use of the device as a nonvolatile memory. Fig. 21 shows the simulated *I–V* characteristics for NMOS and FEMFET received by sweeping the gate voltage from zero to saturation and vice versa. The bulk voltage was set to 0.5 V, the drain voltage to 0.1 V. With a flat hysteresis curve we received a voltage shift of 0.1 V. Caused by the device's built-in potential, the initial polarization for the increasing branch was not zero at gate voltage 0 V, but was pointing into the negative direction. For the decreasing branch the simulation started at the highest applied voltage, so this initial condition was not considered. The hysteresis parameters were selected in a way that saturation was not reached during the simulation, so the up and down curves do not merge in this plot as might be expected.

V. Conclusion

We presented a new algorithm for solving 2-D hysteresis problems, which allows the simulation of devices with arbitrary geometry. This algorithm is capable to reproduce rotational effects and allows the calculation of transfer characteristics. Furthermore, it allows the extraction of effective material parameters for a new class of nonvolatile memory cells.

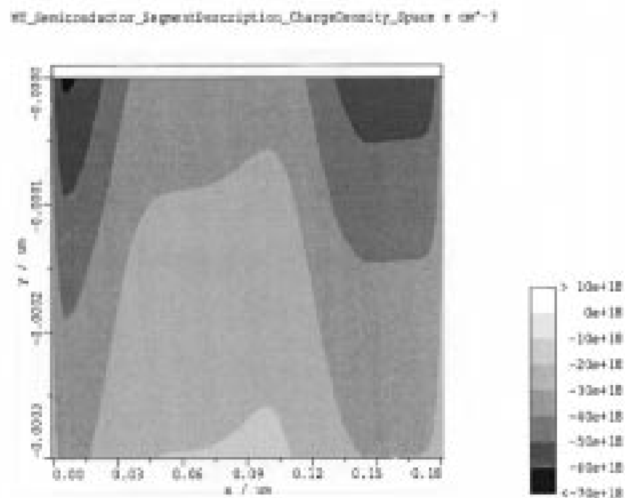

Fig. 19. Space-charge density of the NMOS.

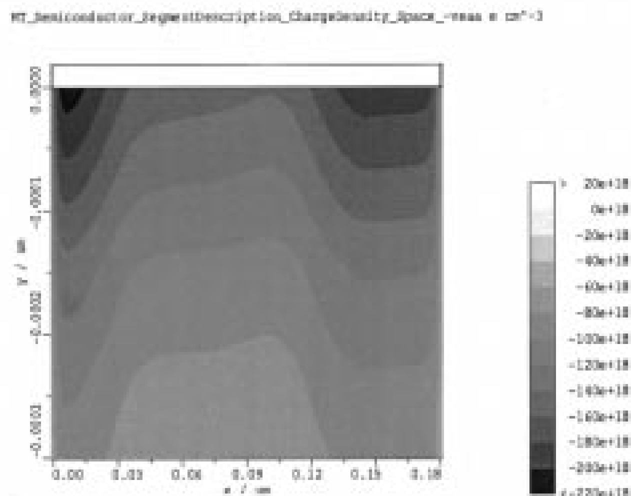

Fig. 20. Space-charge density of the FEMFET.

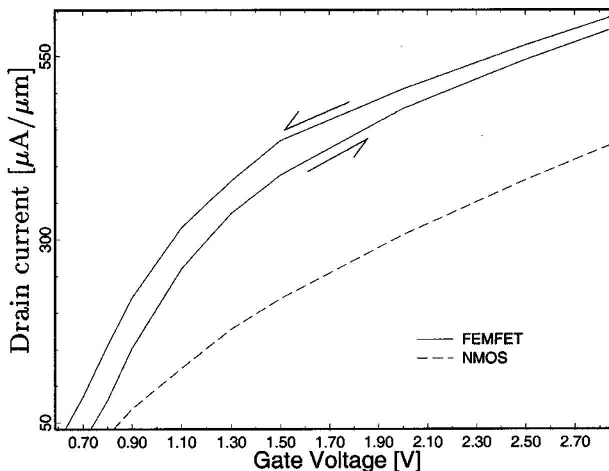

Fig. 21. *I–V* characteristic of FEMFET and NMOS.

ACKNOWLEDGMENT

The authors acknowledge R. Kosik and V. Palankovski for fruitful discussions, and to Dr. T. Grasser for his work on MINIMOS-NT.

REFERENCES

[1] *MINIMOS-NT User's Guide*, Inst. Mikroelektron., Tech. Univ.,, Vienna, Austria, 1998.

[2] H. Pfützner, "Rotational magnetization and rotational losses of grain oriented silicon steel sheets—fundamental aspects and theory," *IEEE Trans. Magn.*, vol. 30, pp. 2802–2807, Sept. 1994.

[3] P. Weiss and V. Planer, "Hysterese dans les champs tournants," *J. Phys.*, vol. 4/7, pp. 5–27, 1908.

[4] B. Jiang *et al.*, "Computationally efficient ferroelectric capacitor model for circuit simulation," in *IEEE Symp. VLSI Technology Dig. Tech. Papers*, 1997, pp. 141–142.

[5] C. Fischer, "Bauelementsimulation in einer computergestützten Entwurfsumgebung," Ph.D. dissertation, Tech. Univ. Wien, Austria, 1994.

[6] I. D. Mayergoyz, *Mathematical Models of Hysteresis*. Berlin, Germany: Springer Verlag, 1991.

Klaus Dragosits was born in Bruck an der Mur, Austria, in 1969. He studied electrical engineering at the University of Vienna, Austria, where he received the Dipl.ing. degree in 1996. He is currently pursuing the Ph.D. degree at the Institute of Microelectronics, Technische Universität Wien, Vienna.

His scientific interests include device simulation with special emphasis on nonvolatile memory cells.

Siegfried Selberherr (F'93) was born in Klosterneuburg, Austria, in 1955. He received the Dipl.ing. degree in electrical engineering and the Ph.D. degree in technical sciences from the Technische Universität Wien (TU), Vienna, Austria, in 1978 and 1981, respectively.

Since then, he has been with TU as a Professor. He has held the *venia docendi* on computer-aided design since 1984. He has been the head of the Institute of Microelectronics, TU, since 1988. His current topics are modeling and simulation of problems for microelectronics engineering.